Available online at www.sciencedirect.com
SCIENCE DIRECT®
Inorganica Chimica Acta 353 (2003) 99–106
Inorganica Chimica Acta
www.elsevier.com/locate/ica

New palladium complexes with bis(8-thiotheophylline)alkane derivatives

Antonio Romerosa [a,*], Carlos López-Magaña [a], Andrés E. Goeta [b], Sonia Mañas [a], Mustapha Saoud [a,c], F.B. Benabdelouahab [c], F. El Guemmout [c]

[a] Área de Química Inorgánica, Facultad de Ciencias Experimentales, Universidad de Almería, 04071 Almería, Spain
[b] Department of Chemistry, University Science Laboratories, South Road, Durham DH1 3LE, UK
[c] Faculty of Sciences-Tetouan, University Abdelmalek Essaadi, B.P. 2121 Tetouan, Morocco

Received 23 October 2002; accepted 24 January 2003

Abstract

Aiming at finding new models that allow us to obtain more information about the interaction between metals and purine-biomolecules, the new derivatives bis(*S*-8-thiotheophylline)methane ($MBTTH_2$) (**1**), 1,2-bis(*S*-8-thiotheophylline)ethane ($EBTTH_2$) (**2**), 1,3-bis(*S*-8-thiotheophylline)propane ($PBTTH_2$) (**3**) and, 1,10-bis(*S*-8-thiotheophylline)decane ($DBTTH_2$) (**4**) were synthesised. The evaluation of the coordinative properties of these new ligands against *cis*-$[PdCl_2(PPh_3)_2]$, leaded to the synthesis of the complexes *trans*-$[PdCl(PPh_3)_2LH]$ ($L = EBTT^{2-}$ (**5**), $PBTT^{2-}$ (**6**)) and *trans*-$[(PdCl(PPh_3)_2)_2L]$ ($L = MBTT^{2-}$ (**7**), $EBTT^{2-}$ (**8**), $PBTT^{2-}$ (**9**), $DBTT^{2-}$ (**10**)). All of the ligands and complexes were characterised by elemental analysis, IR and multinuclear (^1H, $^{13}C\{^1H\}$, $^{31}P\{^1H\}$ NMR) spectroscopy. The crystal structure of the ligand **1** is also presented, confirming the proposed composition for the new purine derivatives.

Keywords: Palladium complexes; Purine derivatives; Metal–purine interaction; Bioinorganic chemistry; Metal–phosphine complexes

1. Introduction

The interaction between metal ions and purine bases is a continuous and important area of study due to the fact that purine bases are the principal constituents of nucleic acid derivatives [1,2]. Purines possess a variety of potential donor groups in their molecular skeleton and consequently behave as effective ligands towards a wide range of metal ions. Coordination to a metal ion largely affects the main chemical properties of the purine molecules [3,4] and, therefore, to know how the natural behaviour of these compounds is changed upon metal-coordination is of paramount importance.

Since the discovery of the cytotoxic activity of cisplatin, *cis*-$[Pt(NH_3)_2Cl_2]$, much effort has been directed towards elucidating the mechanism of action of this drug. At present, it is generally accepted [5] that intracellular damage occurs by coordination of cisplatin to DNA, causing a spatial disturbance and destabilisation of the double-helix leading to inhibition of the DNA replication. The molecular mechanistic aspects of platinum antitumour drugs are commonly investigated by elucidation of the 3D structures for metal adducts of oligonucleotides [6–8]. The construction of selectively metalled DNA adducts by modification of an unprotected oligonucleotide with a metal complex is often hampered by lack of selectivity of the metallation reaction. Consequently, the available range of DNA–Metal crosslinks to be studied is rather limited. One approach to overcome these problems entails the use of models to simplify the parameters to study.

The 8-thio-purine derivatives containing purine bases arranged at different distances to each other, are thought to be adequate models to evaluate the metal coordination properties of the different purine molecules and the influence of the bridge nature. Herein we present the synthesis and characterisation of the new purine derivatives (Scheme 1) bis(*S*-8-thiotheophyl-

* Corresponding author. Tel./fax: +34-950-01 5008.
E-mail address: romerosa@ual.es (A. Romerosa).

0020-1693/03/$ - see front matter © 2003 Elsevier B.V. All rights reserved.
doi:10.1016/S0020-1693(03)00234-2

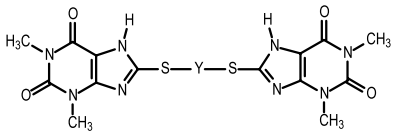

Scheme 1. Y = $-CH_2-$ (**1**, $MBTTH_2$); $-(CH_2)_2-$ (**2**, $EBTTH_2$); $-(CH_2)_3-$ (**3**, $PBTTH_2$); $-(CH_2)_{10}-$ (**4**, $DBTTH_2$).

line)methane ($MBTTH_2$) (**1**), 1,2-bis(*S*-8-thiotheophylline)ethane ($EBTTH_2$) (**2**), 1,3-bis(*S*-8-thiotheophylline)propane ($PBTTH_2$) (**3**) and, 1,10-bis(*S*-8-thiotheophylline)decane ($DBTTH_2$) (**4**). We have evaluated their coordinative properties by reaction with the palladium complex *cis*-$[PdCl_2(PPh_3)_2]$. This metal complex is geometrically similar to the *cis*-$[PtCl_2(NH_3)_2]$, the Pd is thermodynamically similar to Pt, and the presence of two PPh_3 ancillary ligands makes not only the palladium complexes soluble in common organic solvent but provide also a NMR-active label, the P-nucleus of the phosphine, which allows us to study the reaction with the modified purines by $^{31}P\{^1H\}$ NMR spectroscopy.

2. Results and discussion

Elemental analysis, melting point of the ligand, selected IR absorptions, ^1H, $^{31}P\{^1H\}$ and $^{13}C\{^1H\}$ NMR data for all compounds are collected in Tables 1–5.

2.1. Ligands

The ligands **1**, **2**, **3** and **4** were obtained in refluxing EtOH by reaction of 8-thiotheophylline, KOH and, BrRBr (R = $-CH_2$ for **1**, 1,2-$(CH_2)_2$ for **2**, 1,3-$(CH_2)_3$ for **3**, 1,10-$(CH_2)_{10}$ for **4**) in molar ratio 1:1:0.5 (Scheme 2). The structures of these ligands were unequivocally assigned by elemental analysis and their spectroscopic properties.

The new purine derivatives contain two thiotheophyllines linked by an alkyl group through the purine S atom. The ν(N–H) IR band confirmed for all the ligands the existence of an H bonded to the N7 atom, which was also supported by a broad ^1H NMR resonance at 13.59 ppm for **2**, **3** and **4**, and two wide signals for **1** (13.64, 13.82 ppm). The signals due to the N1–CH_3 and N3–CH_3 groups appeared in a very short range (3.19–3.31 ppm, N1–CH_3; 3.37–3.43 ppm, N3–CH_3).

The two purines in **1** were not magnetically equivalent, which could be consequence of the stacking interaction observed in the crystal structure that would also be present in solution and could account for the different chemical shifts observed for the methyl protons. Variable temperature ^1H NMR experiments preformed in DMSO-d_6 showed free rotation of the molecule at 110 °C. The carbon atoms signals in $^{13}C\{^1H\}$ NMR for the two purines appeared in the same position except that for C5, C6 and C8 atoms.

The alkyl bridge group chemical shifts in ^1H NMR for **2**, **3** and **4**, arose at a field lower than that expected for alkyl groups between –S–R (R = alkyl or aryl), which suggests that the 8-thiotheophylline-*S* atom is a electronic attracting atom bigger than the S–R atom. A variable temperature ^1H NMR experiment was needed to perform the correct assignment of the alkyl bridge for **3** (the S–CH_2- and N3–CH_3 chemical shifts are the same at room temperature), and a ^1H COSY-45 was necessary for **4**. The S-alkyl-S carbon atoms arose in $^{13}C\{^1H\}$ NMR in the expected positions. It is only necessary to point out that a DEPT-135 experiment was required to assign the $^{13}C\{^1H\}$ NMR spectrum for **4**.

Finally, it is important to notice that the C8 chemical shift (approximately 148 ppm) for the four ligands appeared in the range of those found for other S substitued thio-theophylline compounds [9].

Table 1
Analytical results for **1**–**10** (calculated in parenthesis)

	Found (calc.) (%)	Molecular weight	% C	% H	% N	% S
1	$C_{15}H_{16}N_8O_4S_2$	436.41	41.40 (41.28)	3.48 (3.66)	25.45 (25.68)	14.28 (14.67)
2	$C_{16}H_{18}N_8O_4S_2$	462.43	42.81 (42.67)	3.88 (4.00)	24.68 (24.89)	13.85 (14.22)
3	$C_{17}H_{20}N_8O_4S_2$	476.44	43.80 (43.96)	4.40 (4.31)	23.67 (24.14)	13.39 (13.79)
4	$C_{24}H_{34}N_8O_4S_2$	574.51	51.12 (51.23)	6.18 (6.09)	19.78 (19.91)	11.08 (11.39)
5	$C_{52}H_{48}ClN_8O_4P_2PdS_2$	1116.94	56.08 (55.92)	4.18 (4.30)	9.89 (10.0)	5.66 (5.74)
6	$C_{53}H_{50}ClN_8O_4P_2PdS_2$	1130.97	56.49 (56.29)	4.30 (4.43)	9.87 (9.91)	5.48 (5.66)
7	$C_{87}H_{74}Cl_2N_8O_4P_4Pd_2S_2$	1767.36	66.23 (66.05)	3.34 (3.48)	5.34 (5.27)	2.87 (3.01)
8	$C_{88}H_{76}Cl_2N_8O_4P_4Pd_2S_2$	1781.38	59.51 (59.34)	4.19 (4.27)	6.01 (6.29)	3.71 (3.60)
9	$C_{89}H_{78}Cl_2N_8O_4P_4Pd_2S_2$	1795.41	58.86 (58.95)	4.33 (4.45)	6.29 (6.18)	3.73 (3.54)
10	$C_{96}H_{92}Cl_2N_8O_4P_4Pd_2S_2$	1893.60	60.94 (60.84)	4.69 (4.86)	5.86 (5.91)	3.41 (3.38)

Table 2
Selected IR parameters for **1**–**10** (ν in cm^{-1})

	ν(N–H)	ν(C–H, Ph)	ν(C6=O)	ν(C2=O)	ν(C=C)+ν(C=N)	PPh_3 absorptions
1	3119–2547		1707	1651	1549	
2	3117–2689		1706	1649	1603	
					1547	
3	3125–2688		1702	1653	1548	
					1504	
4	3100–2650		1700	1649	1623	
			1680		1605	
5	3071–2875	[a]	1697	1649	1542	1478, 1436, 1003
						745, 704, 690
						518, 507, 499
6	3122–2690	[a]	1699	1648	1547	1479, 1435, 1097
					1539	749, 707, 692
					1533	532, 512, 499
7		3051–2943	1684	1646	1584	1481, 1434, 1096
					1527	743, 706, 691
						520, 511, 495
8		3051–2943	1686	1646	1585	1481, 1434, 1096
					1527	743, 706, 691
						519, 512, 493
9		3053–2939	1685	1648	1585	1481, 1434, 1097
					1526	745, 707, 692
						521, 511, 495
10		3065–2850	1705	1657	1543	1479, 1435, 1418
			1693	1648		755, 745, 693
						533, 510, 496

[a] Included into ν(N–H).

2.2. Crystal structure of 8-$MBTTH_2$ (*1*)

In order to confirm the structural composition of the ligand synthesised and to collect novel geometrical information on this class of compounds, an X-ray analysis was carried out on a single crystal of **1** that was obtained from a solution in EtOH–hexane (1:1) by slow evaporation. An ORTEP drawing of the complex is shown in Fig. 1 with the atomic numbering scheme.

One molecule of 8-$MBTTH_2$ constitutes the lattice asymmetric unit, the two 8-thiotheophyllines (A, B) being linked by a methylene group through the S atom. Both purine bases are planar, the angle between mean imidazolic (A rms: 0.008; B rms: 0.003) and pyrimidine

Table 3
^{1}H NMR parameters for **1**–**10** (δ in ppm, J in Hz **1**–**7** recorded in DMSO-d_6, **8**–**10** recorded in $CDCl_3$)

	T (°C)	N1–CH_3	N3–CH_3	N7–H	S–CH_2	P–Ph_3	S–CH_2–CH_2–	S–$(CH_2)_2$–CH_2–	S–$(CH_2)_3$–$(CH_2)_4$–
1	22	3.31	3.43	13.82	5.12(s)				
	80	3.27	3.40	13.64					
		3.33	3.46	13.54 [a]	5.14(s)				
		3.30	3.43						
2	22	3.24	3.37	13.59	3.59(s)				
	80	3.32	3.46	13.49	3.67(s)				
3	22	3.26	3.40	13.59 [a]	3.40		2.17 (c, $J = 6.7$ Hz)		
	40	3.30	3.42	13.54 [a]	3.41 (t, $J = 6.9$ Hz)		2.18 (c, $J = 6.8$ Hz)		
	100	3.31	3.47		3.42 (t, $J = 6.9$ Hz)		2.22 (c, $J = 6.8$ Hz)		
4	22	3.19	3.37	13.59 [a]	3.13 (t, $J = 6.7$ Hz)		1.62 (q, $J = 6.4$ Hz)	1.34(m)	1.22(m)
5	22	3.21	3.33	13.58 [a]	3.57	7.65–7.24			
	50	3.23	3.36	13.46 [a]		7.63–7.28			
6	22	3.19	3.32	13.54 [a]	3.29 (t, $J = 7.0$ Hz)	7.63–7.25	2.08 (q, $J = 6.8$ Hz)		
	50	3.21	3.36	13.42 [a]	3.32 (t, $J = 7.1$ Hz)	7.64–7.28	2.10 (q, $J = 6.8$ Hz)		
7	22	3.15	3.17		4.15	7.74–7.37			
8	22	3.21	3.22		2.87	7.77–7.28			
9	22	3.16	3.18		3.72 (t, $J = 6.9$ Hz)	7.76–7.27	2.56 (q, $J = 6.9$ Hz)		
10	22	3.29	3.42		3.23 (t, $J = 7.0$ Hz)	7.63–7.11	1.46 (m)	1.26 [a]	1.18 (m)

[a] Broad signal.

Table 4
$^{13}C\{^1H\}$ parameters for **1**–**10** (δ in ppm **1**–**7** recorded in DMSO-d_6, **8**–**9** recorded in $CDCl_3$)

	C2	*C4*	*C5*	*C6*	*C8*	N1–*C*H$_3$	N3–*C*H$_3$	S–*C*H$_2$–	S–*C*H$_2$–CH$_2$–	*Ph*	S–(CH$_2$)$_2$–*C*H$_2$–	S–(CH$_2$)$_3$–*C*H$_2$–	S–(CH$_2$)$_4$–CH$_2$–
1	153.2	145.3	108.2	150.8	148.2	27.6	29.6	32.0					
			107.8	150.6	147.8								
2	153.1	147.6	107.8	150.7	148.1	27.6	29.5	32.0					
3	153.0	148.0	107.6	150.7	148.2	27.5	29.4	30.2	29.2				
4	154.3	149.3	110.0	151.5	150.1	30.1	28.0	31.8	29.6		29.2	28.6	28.2
5	153.3	147.8	107.9	150.9	148.2	27.7	29.7	32.0		134.5–128.3			
6	154.6	148.5	111.7	153.2	150.8	27.7	29.8	30.7	29.3	134.2–127.2			
		148.2	107.6	151.9	149.7	27.4	29.6	30.1	29.0				
7	154.6	149.8	111.4	150.5	150.3	27.4	29.0	36.9		134.1–128.1			
8	154.8	150.3	112.2	151.5	150.9	27.6	29.2	32.7		134.6–128.0			
9	154.7	150.3	112.0	151.5	151.0	27.6	29.1	30.4	28.6	134.6–128.0			
10 [a]													

[a] No soluble enough.

Table 5
$^{31}P\{^1H\}$ parameters for **5**–**10** (δ in ppm **5**–**7** recorded in DMSO-d_6, **8**–**10** recorded in $CDCl_3$)

	δ (T^a Amb)		δ (T^a 40 °C)	
5	38.10	10.57%	37.98	8.13%
	32.65	5.80%	27.51	66.25%
	31.58	4.72%	27.36	16.45%
	29.56	58.61%	26.90	9.17%
	27.40	14.52%		
	26.98	5.78%		
6	25.04	100%		
7	22.80	100%		
8	22.38	100%		
9	17.35	100%		
10	21.62	100%		

(A rms: 0.007; B rms: 0.001) planes for purines A and B being 2.36(6) and 1.95(7)°, respectively. The exocyclic purine groups are fitted with the pyrimidine base plane, the greater deviation being for C3A atom (0.057(1) Å).

The two purine bases are in a parallel disposition (angle between imidazolic purine planes = 5.46(7)°), with similar exocyclic groups situated as far as possible to each other. The shortest distance between the two purines (C6A–N3B = 3.53(18) Å) is longer than the sum of the radii of the atoms [10]. It is clear from the molecular structure that a stacking interaction is present between the two linked 8-thiotheophylline units of compound **1**.

The C8–S bond length is the same within e.s.d.s in both purines (C8A–S1A = 1.7476(19) Å; C8B–S1B = 1.7490(19) Å) and significantly shorter than the S1–C10 bond length (S1A–C10 = 1.816(2) Å; S1B–C10 = 1.807(2) Å). Finally, bond distances and angles are similar to those found in other purine molecules [11–16] and there are no significant interactions between molecules.

2.3. Palladium complexes

All the complexes synthesised by reaction of the ligands **1**–**4** with *cis*-$[PdCl_2(PPh_3)_2]$ (or 2 mol PPh_3 + 1 mol $[PdCl_4]^{2-}$ in 3 ml of H_2O) (Scheme 3) were coordinated through the N7 imidazolic atom to the palladium atom of the unit $[PdCl(PPh_3)_2]^+$. Reacting 1 mol of the new purine derivatives **2** and **3** with 1 mol of KOH and 1 mol of *cis*-$[PdCl_2(PPh_3)_2]$ (or 2 mol PPh_3 + 1 mol $[PdCl_4]^{2-}$ in 3 ml of H_2O) the complexes **5** and **6** were obtained. In these complexes the metal coordinated to a single purine, the other purine resting protonated. The complexes **8** and **9**, were obtained using a 1:2:2 ligand/KOH/metal molar ratio, or by reaction of complexes **5** and **6** with 1 mol of KOH and 1 mol of *cis*-$[PdCl_2(PPh_3)_2]$ (or 2 mol PPh_3 + 1 mol $[PdCl_4]^{2-}$ in 3 ml of H_2O). The complexes **7** and **10**, were obtained by reaction of **1** and **4** with KOH and *cis*-$[PdCl_2(PPh_3)_2]$

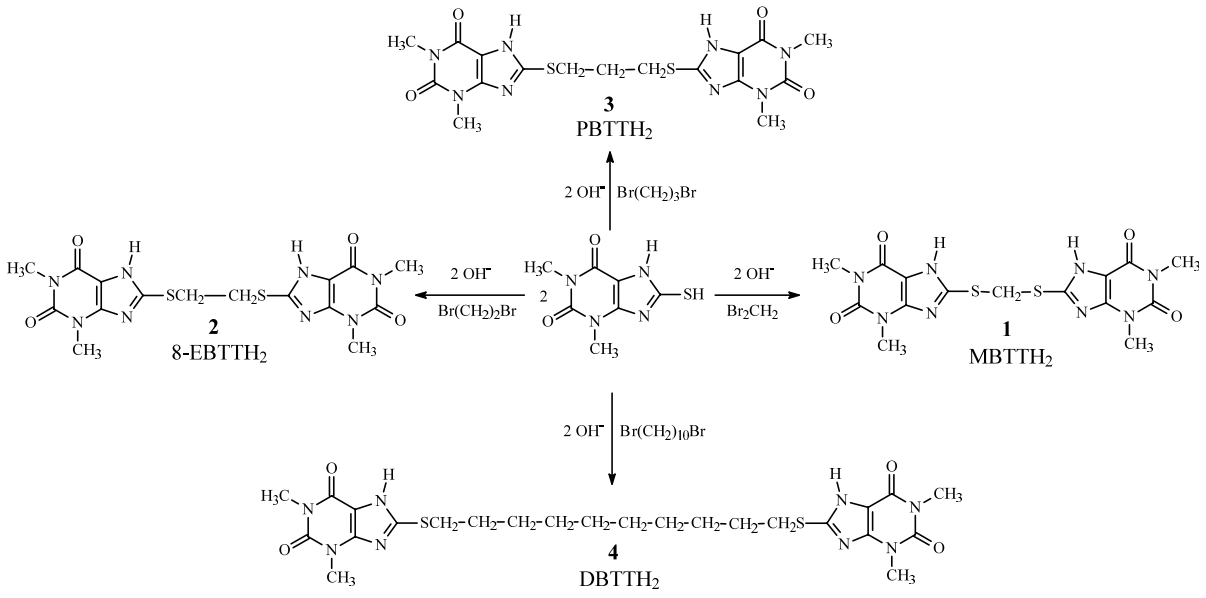

Scheme 2.

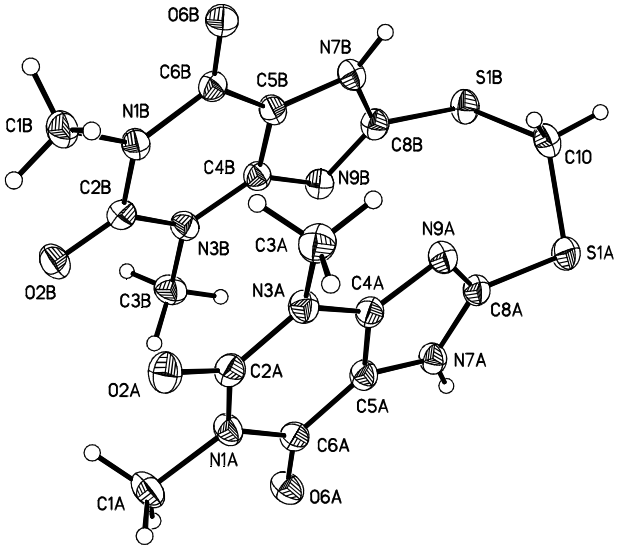

Fig. 1. Molecular diagram of the ligand **1**.

(or PPh_3 + mol $[PdCl_4]^{2-}$ in 3 ml of H_2O) in any molar ratio but the best yield was obtained for 1:2:2 ligands/KOH/metal molar ratio.

All of the complexes were clearly characterised by elemental analysis, IR and NMR spectroscopy. According to their spectroscopic properties the palladium complexes could be classified by those in which a single purine was only bonded to the metal, $[PdCl(PPh_3)_2LH]$ ($L = EBTT^{2-}$ (**5**), $PBTT^{2-}$ (**6**)), and those in which the two purines were coordinated to metal, $[(PdCl(PPh_3)_2)_2L]$ ($L = MBTT^{2-}$ (**7**), $EBTT^{2-}$ (**8**), $PBTT^{2-}$ (**9**), $DBTT^{2-}$ (**10**)).

The main characteristic difference in the IR spectrum between the two classes of palladium complexes is the ν(NH) that is only observed in those containing a free purine, complexes **5** and **6**. The ν(C6=O) and ν(C2=O) frequency are similar in all complexes (mean ν(C6=O) = 1693(12) cm^{-1}; mean ν(C2=O) = 1649(8) cm^{-1}) and very similar to those found for the free ligand (mean ν(C6=O) = 1699(19) cm^{-1}; mean ν(C2=O) = 1650(3) cm^{-1}), being therefore no useful to characterise the complexes. The existence of N7–H atom is supported by the broad signal observed on 13 ppm in ^1H NMR. There are no differences between the N1–CH_3 and N3–CH_3 resonances of the purine bound to Pd and those of the protonated purine. That fact is not peculiar for that kind of ligands and complexes [11–16].

The resonances of the N1–CH_3 and N3–CH_3 arose in a similar chemical shift for all complexes (mean δ N1–CH_3 = 3.20(9) ppm; δ N3–CH_3 = 3.27(15) ppm) and very close to those observed for the ligands (mean δ N1–CH_3 = 3.25(6) ppm; δ N3–CH_3 = 3.39(4) ppm). A correlation among the ligand, the composition of the complexes and the chemical shifts of the bridge alkyl groups, was not found. The $^{13}C\{^1H\}$ NMR spectrum of the complexes showed no significant chemical shift changes by ligand coordination.

Finally, the chemical shift (< 30 ppm) of the $^{31}P\{^1H\}$ NMR signals for all complexes indicated that the two PPh_3 groups were *trans* to each others [17,18]. The **6**, **7**, **8**, **9** and **10** $^{31}P\{^1H\}$ NMR spectrums exhibited a single signal in the range from −60 to 60 °C. In contrast, **5** was only soluble in DMSO-d_6. In that solvent the complex was in equilibrium among at least six different species at room temperature that became 4 ones at 40 °C. Complex **5** was again and again obtained (four times) from DMSO solution by evaporation (yield 100%) or precipitation with hexane (yield 95%). Unfortunately, the determination of the nature of the different species in solution was not possible.

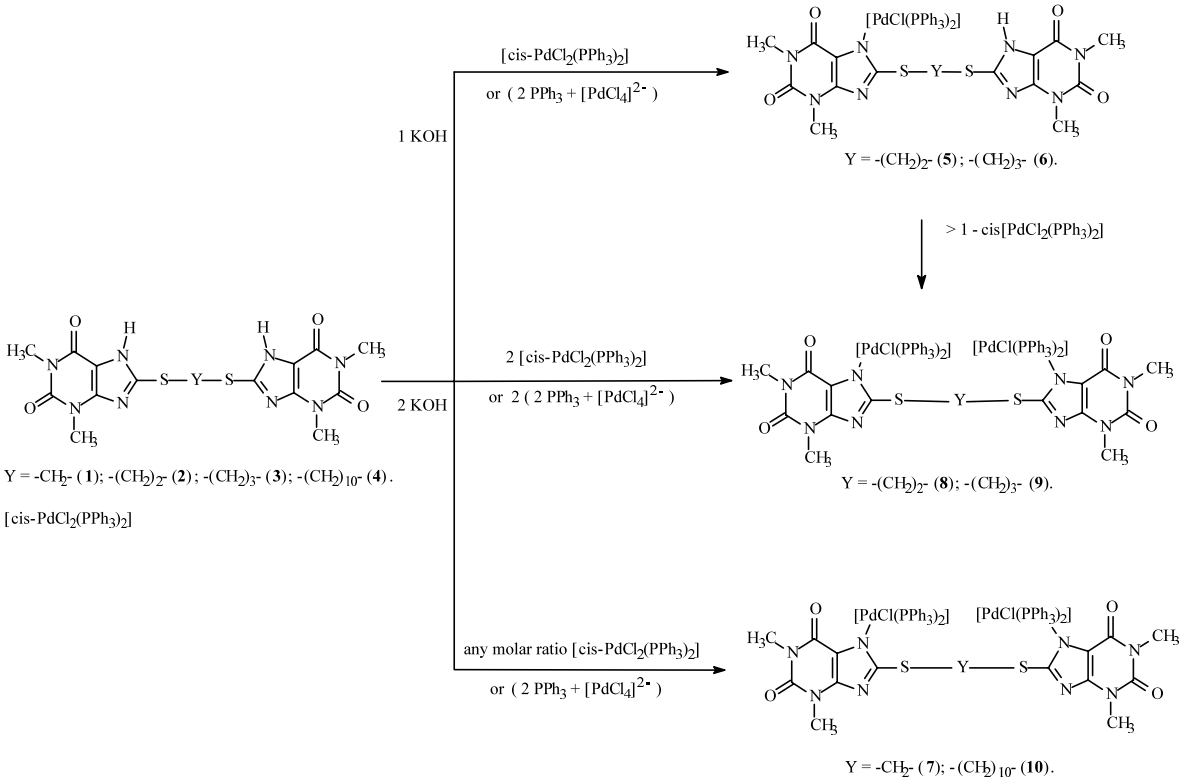

Scheme 3.

3. Conclusion

We have synthesised four new theophylline derivatives in which two 8-thiotheophylline groups are linked by an alkyl group through the S atom, bis(*S*-8-thiotheophylline)methane ($MBTTH_2$) (**1**), 1,2-bis(*S*-8-thiotheophylline)ethane ($EBTTH_2$) (**2**), 1,3-bis(*S*-8-thiotheophylline)propane ($PBTTH_2$) (**3**), and 1,10-bis(*S*-8-thiotheophylline)decane ($DBTTH_2$) (**4**). We have synthesised their palladium complexes $[PdCl(PPh_3)_2LH]$ ($L = EBTT^{2-}$ (**5**), $PBTT^{2-}$ (**6**)) and $[(PdCl(PPh_3)_2)_2L]$ ($L = MBTT^{2-}$ (**7**), $EBTT^{2-}$ (**8**), $PBTT^{2-}$ (**9**), $DBTT^{2-}$ (**10**)). We have not observed the formation of the complexes $[(PdCl(PPh_3)_2)_2LH]$ ($L = MBTT^{2-}$, $DBTT^{2-}$). The palladium complexes coordination purine site was found to be the N7 imidazolic atom, being also coordinated to two PPh_3 *trans* to each other and to a chloride atom *trans* to the purine N7 atom. The most probable metal coordination geometry is squared-planar. Cleavage of the C8–S bond was never observed. For ligands **2** and **3** a selective control of the ligand purine coordination according to the reagents molar ratio was possible. The compounds **1**–**4** can be used such as macrochelate ligands. Finally, on the basis of the results obtained the study of the reaction of the new purine derivatives with Pt and Ru complexes is in progress with the aim of elucidating the possible reason of the different ligand coordinative behaviour.

4. Experimental

All reagents were of analytical grade and were used without further purification. The complexes *cis*-$[PdCl_2(PPh_3)_2]$[6], $Na_2[PdCl_4]$[6] and the ligand 8-thiotheophylline [19] were prepared as described previously. Experiments were routinely prepared under argon by using standard Schlenk-tube techniques. Deuterated solvents for NMR measurements were dried over molecular sieves (0.4 nm). ^1H, $^{13}C\{^1H\}$ and $^{31}P\{^1H\}$ NMR spectra were recorded on a Bruker AVANCE DRX 300 spectrometer. Peak positions are relative to Me_4Si (^1H, $^{13}C\{^1H\}$) and were calibrated with respect to the residual protonated solvent (^1H) or to the solvent resonance (^{13}C). The $^{31}P\{^1H\}$ NMR spectra are given with respect to external 85% H_3PO_4 in D_2O with downfield values taken as positive. Infrared spectra were recorded (on KBr discs) on a IR-ATI Mattson Infinity Series. Elemental analysis (C, H, N, S) was performed on a Fisons Instruments EA 1108 elemental analyser. Melting points were recorded on a BÜCHI 530 instrument.

5. X-ray crystallography

The colourless crystal used for X-ray work ($0.42 \times 0.18 \times 0.16$ mm) was obtained from a solution of **1** in ethanol–hexane (1:1) by slow evaporation of the sol-

vent. Single crystal structure determination of **1** was carried out at 120 K from data collected using graphite monochromated Mo Kα radiation ($\lambda = 0.71073$) on a Bruker SMART-CCD 1K detector diffractometer equipped with a Cryostream N2 flow cooling device [20]. Series of narrow ω-scans (0.3°) were performed at several ϕ-settings in such a way as to cover a sphere of data to a maximum resolution of 0.70 Å. Cell parameters were determined and refined using the SMART software [21] from the centroid values of 625 reflections with 2θ values between 27 and 49°. Raw frame data were integrated using the SAINT program [22]. The structure was solved using Direct Methods and refined by full-matrix least-squares on F^2 using SHELXTL [23]. No absorption correction was applied to the data.

The compound crystallizes in the orthorhombic system, space group *Pbca*, with $a = 12.447(4)$, $b = 13.585(5)$, $c = 21.038(7)$ Å, $U = 3557(2)$ Å^3, $Z = 8$, $D_c = 1.630$ g cm^{-3} and $\mu = 0.345$ mm^{-1}. 41 294 reflections were collected and 5175 unique reflections ($R_{int} = 0.0486$) were used in all calculations ($2\theta_{max} = 60.94$, $h = -17$–16, $k = -18$–19, $l = -28$–29). From these, 3817 reflections were considered 'observed' ($I > 2\sigma(I)$). The final wR (F^2) was 0.1241 (all data) and the final R (F) was 0.045 (observed data). All non-hydrogen atoms were refined with anisotropic atomic displacement parameters (adps). Hydrogen atoms were geometrically placed and allowed to ride on their parent C atoms with U_{iso} (H) = 1.5 U_{eq}(C) for methyl H atoms, and 1.2 U_{eq}(C) for the methylene group. Idealized C–H distances were fixed at 0.98 and 0.99 Å, respectively. Hydrogen atoms bonded to N atoms were located from a difference Fourier map and its coordinates and isotropic adps were refined.

6. Preparation

Synthesis of bis(*S*-8-thiotheophylline)methane (MBTTH$_2$) (**1**), 1,2-bis(*S*-8-thiotheophylline)ethane (EBTTH$_2$) (**2**), 1,3-bis(*S*-8-thiotheophylline)propane (**3**), 1,10-bis(*S*-8-thiotheophylline)decane (DBTTH$_2$) (**4**).

The ligands **1**, **2**, **3** and **4** were obtained by a similar procedure. Into a suspension of potassium 8-thiotheophyllinate in 20 ml of EtOH, which was generated in situ by reaction of 8-thiotheophylline (1 g, 5 mmol) with KOH (0.28 g, 5 mmol), the respective dibromoalkyl derivative, BrRBr (R = –CH$_2$ for **1**, 1,2-(CH$_2$)$_2$ for **2**, 1,3-(CH$_2$)$_3$ for **3**, 1,10-(CH$_2$)$_{10}$ for **4**), was added. The mix was stirred for 30 min at room temperature and then refluxed for 6 h. The yellow solution was slowly cooled and finally kept in a freezer all night. The white–yellow powder precipitated was filtered out, washed with H$_2$O (2 × 2 ml), EtOH (2 × 2ml) and air dried.

Pale yellow crystals of **1** were obtained from a solution in EtOH/hexane (1:1) by slow evaporation at room temperature.

Yield **1**: 86%, 1.87 gYield **2**: 84%, 1.94 g;Yield **3**: 64%, 1.52 g;Yield **4**: 76%, 2.18 g.Melting point **1**: 298–299 °C;Melting point **2**: 312–313 °C;Melting point **3**: 253–254 °C;Melting point **4**: 261–262 °C.

6.1. Synthesis of trans-[PdCl(PPh$_3$)$_2$LH] (L = EBTT^{2-} (**5**), PBTT^{2-} (**6**))

By a similar procedure, **2** (0.46 g, 1 mmol) and **3** (0.47 g, 1 mmol) reacted with KOH (0.056 g, 1 mmol) and *cis*-[PdCl$_2$(PPh$_3$)$_2$] (0.70 g, 1 mmol) for 2 h in refluxed EtOH (15 ml) to give rise the complexes **5** and **6** as red orange precipitates, which were filtered out, washed with two portions of cold EtOH and air dried.

The complexes could be also obtained by previous deprotonation of **2** (0.46 g, 1 mmol) and **3** (0.47 g, 1 mmol) with KOH (0.1 mol) in 15 ml of EtOH and, at refluxed temperature, further reaction with PPh$_3$ (0.2 mol) and Na$_2$[PdCl$_4$] (0.29 g, 1 mmol) dissolved in 3 ml of H$_2$O.

Yield **5**: 44%, 0.49 g;Yield **6**: 47%, 0.53 g.

6.2. Synthesis of the complex trans-[(PdCl(PPh$_3$)$_2$)$_2$L] (L = MBTT^{2-} (**7**), EBTT^{2-} (**8**), PBTT^{2-} (**9**), DBTT^{2-} (**10**))

The complexes **7**, **8**, **9** and **10** were obtained by reaction of the respective ligand **1** (0.43 g, 1 mmol), **2** (0.46, 1 mmol), **3** (0.47 g, 1 mmol) and **4** (0.53 g, 1 mmol) with KOH (0.12 g, 2.2 mmol) and *cis*-[PdCl$_2$(PPh$_3$)$_2$] (1.54 g, 2.2 mmol) (or PPh$_3$ (1.15 g, 4.4 mmol) + Na$_2$[PdCl$_4$] (0.64 g, 2.2 mmol) solved in 3 ml of H$_2$O) in 15 ml of refluxing EtOH. The orange-red precipitated formed after 3 h was filtered out, washed with EtOH (2 × 2 ml) and air dried.

The complexes **8**, **9** were also obtained by refluxing for 2 h the respective complexes **5** (1.12 g, 1 mmol) and **6** (1.13 g, 1 mmol) with KOH (0.056 g, 1 mmol) and *cis*-[PdCl$_2$(PPh$_3$)$_2$] (0.77, 1.1 mmol) (or PPh$_3$ (0.58 g, 2.2 mmol) + Na$_2$[PdCl$_4$] (0.32 g, 1.1 mmol) solved in 3 ml of H$_2$O) in 10 ml of EtOH. The orange–red precipitated obtained was isolated with a similar procedure that described previously.

Yield **7**: 35%, 0.62 gYield **8**: 65%, 1.16 g;Yield **9**: 65%, 1.17 g;Yield **10**: 40%, 0.76 g.

7. Supplementary material

Tables 1, 2 and 5 are included in the supplementary materials. Crystallographic data for the structural analysis have been deposited with the Cambridge Crystallographic Data Centre, CCDC No. 201319. Copies of this information may be obtained free of charge from http://www.ccdc.cam.ac.uk/conts/retrieving.html or from The Director, CCDC, 12 Union Road, Cambridge, CB2 1EZ, UK (fax: +44-1223-336-033; e-mail: deposit@ccdc.cam.ac.uk or www: http://www.ccdc.cam.ac.uk).

Acknowledgements

Thanks are due to the bilateral projects 'Programa Hispano-Marroquí' (AECI, MAE, 1P/97, 21PRO/98 y 21PRO/99) and ''Conserjería de la Presidencia. Junta de Andalucía'' (Project A29/00) for supporting the stay of M.S. in Almería.

References

[1] B. Lippert, Coord. Chem. Rev. 200 (2000) 487.
[2] A. Sigel, H. Sigel (Eds.), Metal Ions in Biological Systems, vol. 32, Marcel Dekker, New York, 1996, p. 1.
[3] U. Bierbach, N. Farrell, Inorg. Chem. 36 (1997) 3657.
[4] Z. Guo, P.J. Sadler, Angew. Chem. Int. Ed. 38 (1999) 1513.
[5] J. Reedijk, Chem. Commun. (1996) 801.
[6] P.M. Takahara, A.C. Rosenzaweig, C.A. Frederick, S.J. Lippard, Nature 377 (1995) 649.
[7] A. Gelasco, S.J. Lippard, Biochem. 37 (1998) 9230.
[8] B.A. Jansen, J. van der Zwan, H. den Dulk, J. Brouwer, J. Reedijk, J. Med. Chem. 44 (2) (2001) 245.
[9] A. Romerosa, C. López-Magaña, M. Saoud, E. Colacio, J. Suarez-Varela, Inorg. Chim. Acta 307 (2000) 125.
[10] A.G. Orpen, L. Brammer, J. Chem. Soc., Dalton Trans. (1989) S1.
[11] E. Freisinger, S. Meier, B. Lippert, J. Chem. Soc., Dalton Trans. (2000) 3274.
[12] E. Alessio, E. Iengo, E. Zangrado, S. Geremia, P.A. Marzilli, M. Calligaris, Eur. J. Inorg. Chem. (2000) 2207.
[13] E. Colacio, A. Romerosa, J. Ruiz, P. Roman, J.M. Gutierrez-Zorrilla, M. Martínez-Ripoll, J. Chem. Soc., Dalton Trans. (1989) 2323.
[14] E. Colacio, A. Romerosa, J. Ruiz, P. Roman, J.M. Gutierrez-Zorrilla, A. Vegas, M. Martínez-Ripoll, Inorg. Chem. 30 (1991) 3743.
[15] E. Colacio, R. Cuesta, J.M. Moreno, Inorg. Chem. 36 (1997) 1084.
[16] E. Colacio, R. Cuesta, M. Ghazi, M.A. Huertas, J.M. Moreno, A. Navarrete, Inorg. Chem. 36 (1997) 1652.
[17] J. Mason, Multinuclear NMR, Plenum Press, New York, 1987.
[18] R. Bruce King, (Ed.), Encyclopedia of Inorganic Chemistry, Wiley, Chichester, 1994.
[19] K.W. Merz, P.H. Sthal, Arzneim.-Forsch. 15 (1965) 10.
[20] J. Cosier, A.M. Glazer, J. Appl. Cryst. 19 (1986) 105.
[21] SMART-NT, Data Collection Software, Version 5.0, Bruker Analytical X-ray Instruments Inc., Madison, WI, 1998.
[22] SAINT-NT, Data Reduction Software, Version 5.0, Bruker Analytical X-ray Instruments Inc., Madison, WI, 1998.
[23] SHELXTL, Version 5.1, Bruker Analytical X-ray Instruments Inc., Madison, WI, 1998.